

# We are IntechOpen, the world's leading publisher of Open Access books Built by scientists, for scientists

4,800

Open access books available

122,000

International authors and editors

135M

Downloads

Our authors are among the

154

Countries delivered to

TOP 1%

most cited scientists

12.2%

Contributors from top 500 universities



WEB OF SCIENCE™

Selection of our books indexed in the Book Citation Index  
in Web of Science™ Core Collection (BKCI)

Interested in publishing with us?  
Contact [book.department@intechopen.com](mailto:book.department@intechopen.com)

Numbers displayed above are based on latest data collected.  
For more information visit [www.intechopen.com](http://www.intechopen.com)



# Convection Flow of MHD Couple Stress Fluid in Vertical Microchannel with Entropy Generation

*Abiodun A. Opanuga, Olasunmbo O. Agboola,  
Hilary I. Okagbue and Sheila A. Bishop*

## Abstract

Entropy generation of fully developed steady, viscous, incompressible couple stress fluid in a vertical micro-porous-channel in the presence of horizontal magnetic field is analysed in this work. The governing equations for the flow are derived, and nondimensionalised and the resulting nonlinear ordinary differential equations are solved via a rapidly convergent technique developed by Zhou. The solution of the velocity and temperature profiles are utilised to obtain the flow irreversibility and Bejan number. The effects of couple stresses, fluid wall interaction parameter (FSIP), effective temperature ratio (ETR), rarefaction and magnetic parameter on the velocity profile, temperature profile, entropy generation and Bejan number are presented and discussed graphically.

**Keywords:** microchannel, entropy generation, MHD, natural convection, differential transform method (DTM)

## 1. Introduction

In the last decades, the study of microchannel flows has become an important subject for researchers because of the reduction in the size of such devices which increases the dissipated heat per unit area. The effective performance of these devices is dependent on the temperature; as a result a comprehensive knowledge of such flow behaviours is required for accurate prediction of performance during the design process. These microfluidics have characteristic lengths of 1 – 100  $\mu\text{m}$  and are categorised by the dimensionless quantity called the Knudsen number ( $Kn$ ). Researchers have shown that microchannel flows are influenced by several parameters of which velocity slip and temperature jump occurring at the solid-fluid interface in small-scale systems are the most important [2–4]. Velocity slip and temperature jump become more significant at higher Knudsen number. The latter boundary conditions are assumed at Knudsen number greater than 0.01 since below this value the classical Navier-Stokes equations is no longer valid.

The influence of velocity slip and temperature jump on microchannel flows has been extensively studied. Khadrawi and Al-Shyyab [5] obtained a close form

solution of the effect of velocity slip and temperature jump on heat and fluid flow for axially moving micro-concentric cylinders. Chen and Tian [6] applied lattice Boltzmann numerical technique with Langmuir model for the velocity slip and temperature jump to investigate fluid flow and heat transfer between two horizontal parallel plates. The study suggested the application of Langmuir-slip model as an alternative for the Maxwell-slip model. Earlier on, Larrode et al. [7] in his work, slip-flow heat transfer in circular tubes, has stated the significance of fluid-wall interaction. Moreover, Adesanya [8] has analytically studied the effects of velocity slip and temperature jump on the unsteady free convective flow of heat-generating/heat-absorbing fluid with buoyancy force. The study concluded that an increase in the slip parameter enhanced fluid motion, while an increase in the temperature jump parameter increased fluid temperature. Aziz and Niedbalski [9] applied finite difference technique to investigate thermally developing microtube gas flow with respect to both radial and axial coordinates. The result indicated that increase in Knudsen number reduced local Nusselt number (Nu). Several investigations regarding microchannel flows have also been carried out by Jha and collaborators [10–12].

From the perspective of energy management, it has been established that thermal processes such as the microscale fluid flow and heat transfer modelling are irreversible. This implies that entropy generation which destroys the available energy leading to inefficiency of thermal designs exists. Therefore, the aim of this research endeavour is the minimisation of irreversibility associated with microchannel flow of couple stress fluid by applying the robust approach proposed by Bejan [13] and applied by numerous researchers such as Adesanya and collaborators [14–16], Adesanya and Makinde [17–18], Ajibade and Jha [19], Eegunjobi and Makinde [20–21], Das and Jana [22] and more recently Opanuga and his collaborators [23–26].

In this work, an efficient technique introduced by Zhou has been employed to construct the solutions of the velocity and temperature profiles. Due to the accuracy of this technique in handling numerous linear and nonlinear models of both ordinary and partial equations, it has gained wide applications by investigators over the last decades. Arikoglu and Ozkol [27] applied it to obtain the solution of difference equations. Biazar and Eslami [28] solved quadratic Riccati differential equation using this method. Agboola et al. [29–30] applied it to third-order ordinary differential equations and natural frequencies of a cantilever beam. Solutions of Volterra integral equation via this technique was obtained by Odibat [31], while Opanuga et al. [32] compared the method with Adomian decomposition method to find the solution of multipoint boundary-value problem and more recently in couple stress fluid model [33].

## **2. Problem formulation**

A fully developed laminar, viscous, incompressible and electrically conducting couple stress fluid in a vertical parallel microchannel of width  $h$  is considered. The  $x$ -axis is such that it is vertically upward along the plates while the  $y$ -axis is taken normal to it. There is an asymmetric heating of the plates such that the hotter plate ( $y = 0$ ) is maintained at temperature  $T_1$ , while the cooler plate ( $y = h$ ) is at temperature  $T_2$ , ( $T_1 > T_2$ ) and  $T_0$  is the reference frame. Velocity slip and temperature jump are incorporated. Furthermore, induced magnetic field effect arising due to the motion of an electrically conducting fluid is taken into consideration (**Figure 1**). Following Cheng and Weng [34], the velocity slip and temperature jump are given as

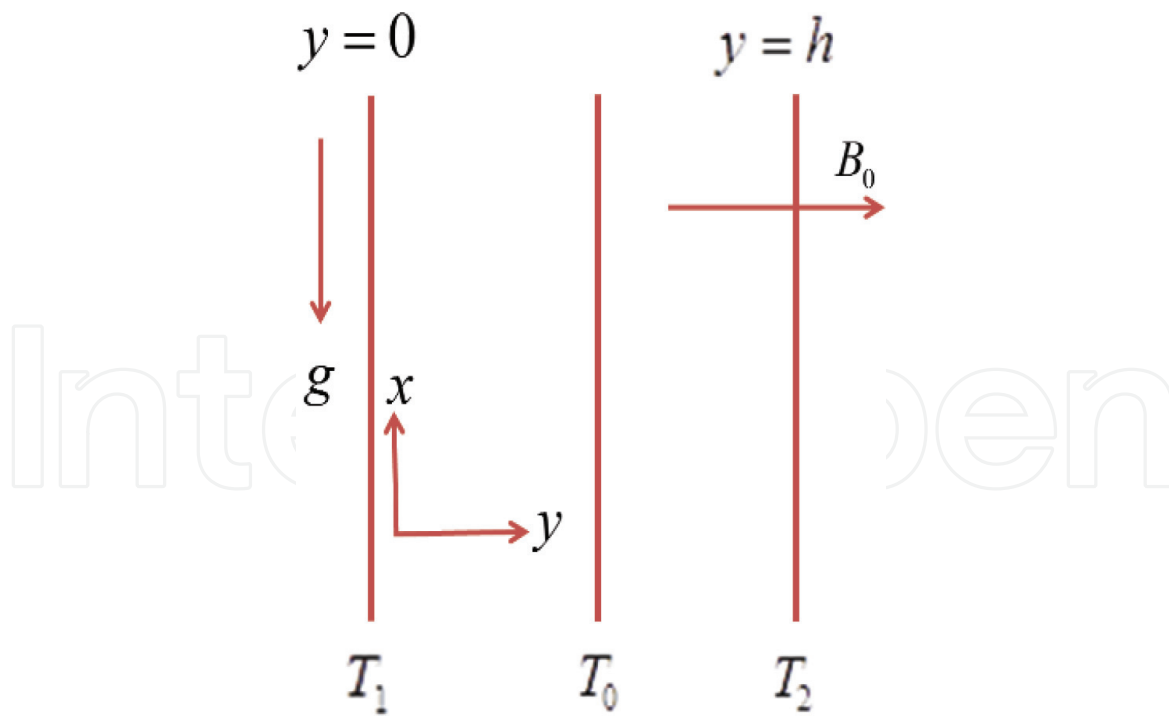


**Figure 1.**  
 Scheme of the vertical microchannel.

$$u_s = -\frac{2 - \sigma_v}{\sigma_v} \lambda \frac{du}{dy'} \Big|_{y'=h}, T_s - T_w = -\frac{2 - \sigma_t}{\sigma_t} \frac{2\gamma}{\gamma + 1} \frac{\lambda}{\text{Pr}} \frac{dT}{dy'} \Big|_{y'=h} \quad (1)$$

While the governing equations for the flow are stated as [10]

$$\rho\nu_* \frac{du'}{dy'} = -\frac{dp}{dx'} + \mu \frac{d^2u'}{dy'^2} - \eta \frac{d^4u'}{dy'^4} + \rho g \beta^* (T - T_0) - \sigma B_0^2 u' \quad (2)$$

$$\rho c_p \nu_0 \frac{dT'}{dy'} = k \frac{d^2T'}{dy'^2} + \mu \left( \frac{du'}{dy'} \right)^2 + \eta \left( \frac{d^2u'}{dy'^2} \right)^2 + \sigma B_0^2 u'^2 \quad (3)$$

The boundary conditions are

$$\begin{aligned} u' &= \frac{2 - f_v}{f_v} \lambda \frac{du'}{dy'}, \frac{d^2u'}{dy'^2} = 0, T' = T_2 + \frac{2 - f_t}{f_t} \frac{2\gamma}{\gamma + 1} \frac{\lambda}{\text{Pr}} \frac{dT'}{dy'}, y = 0 \\ u' &= -\frac{2 - f_v}{f_v} \lambda \frac{du'}{dy'}, \frac{d^2u'}{dy'^2} = 0, T' = T_1 - \frac{2 - f_t}{f_t} \frac{2\gamma}{\gamma + 1} \frac{\lambda}{\text{Pr}} \frac{dT'}{dy'}, y = h \end{aligned} \quad (4)$$

The dimensionless parameters for this flow are

$$\begin{aligned} y &= \frac{y'}{h}, u = \frac{u'}{\nu_*}, \theta = \frac{T' - T_0}{T_1 - T_0}, \text{Re} = \frac{\rho \nu_0 h}{\mu}, G = \frac{-h^2 dp}{\mu \nu_0 dx}, a^2 = \mu \frac{h^2}{\eta}, \\ \text{Pr} &= \frac{\nu \rho c_p}{k}, \text{Br} = \frac{\mu \nu_0}{k(T_1 - T_0)}, \text{Bi}_1 = \frac{\gamma_1 h}{k}, \text{Bi}_2 = \frac{\gamma_2 h}{k}, \nu = \frac{\mu}{\rho}, \\ \Omega &= \frac{T_1 - T_0}{T_0}, H^2 = \frac{\sigma B_0^2 h^2}{\mu}, \xi(T_2 - T_0) = T_1 - T_0, \beta_v = \frac{2 - f_v}{f_v}, \\ \beta_t &= \frac{2 - f_v}{f_v} \frac{2\gamma_s}{\gamma_s + 1} \frac{1}{\text{Pr}}, \gamma_s = \frac{c_p}{c_v}, \text{Kn} = \frac{\lambda}{h}, \psi = \frac{\beta_t}{\beta_v}, \text{Ns} = \frac{S_G T_0 h^2}{k(T_1 - T_0)} \end{aligned} \quad (5)$$

Using (5) in Eqs. (2)–(4) yields the boundary-value problems:

$$\operatorname{Re} \frac{du}{dy} = G + \frac{d^2u}{dy^2} - \frac{1}{a^2} \frac{d^4u}{dy^4} - H^2u + Gr\theta, \quad (6)$$

$$\frac{d^2\theta}{dy^2} = \operatorname{Re} p_r \frac{d\theta}{dy} - Br \left\{ \left( \frac{du}{dy} \right)^2 + \frac{1}{a^2} \left( \frac{d^2u}{dy^2} \right)^2 + H^2u^2 \right\}, \quad (7)$$

$$\begin{aligned} u = \beta_v Kn \frac{du}{dy}, \frac{d^2u}{dy^2} = 0, \theta = \xi + \beta_v Kn \psi \frac{d\theta}{dy}, y = 0 \\ u = -\beta_v Kn \frac{du}{dy}, \frac{d^2u}{dy^2} = 0, \theta = 1 - \beta_v Kn \psi \frac{d\theta}{dy}, y = 1 \end{aligned} \quad (8)$$

### 3. Method of solution

DTM is applied in this work to obtain the solution of the velocity and temperature profiles. The results are used to calculate the entropy generation and irreversibility ratio.

#### 3.1 Differential transformation method (DTM)

Consider a function,  $f(x)$ . The differential transformation of the function  $f(x)$  is defined as

$$F(k) = \frac{1}{k!} \left[ \frac{d^k f(x)}{dx^k} \right]_{x=x_0} \quad (9)$$

where  $f(x)$  is the given function and  $F(k)$  is the transformed function which is also known as the spectrum of  $f(x)$ . The inverse differential transformation of  $F(k)$  is given by

$$f(x) = \sum_{k=0}^{\infty} x^k F(k) \quad (10)$$

In practise, the function stated in Eq. (10) is usually represented by a finite series of the form:

$$f(x) = \sum_{k=0}^n x^k F(k) \quad (11)$$

where  $n$  is the size of the series (Arikoglu and Ozkol [27], Biazar and Eslami [28]).

To apply DTM to the problem in view, the basic properties of DTM, which are outlined in **Table 1**, are invoked in Eqs. (6)–(8). Doing this, one obtains the following recurrence relations:

$$F(k+4) = \frac{1}{a^2(k+4)!} [(k+1)(k+2)F(k+2) - \operatorname{Re}(k+1)F(k+1) - H^2(F(k)) + G] \quad (12)$$

Original function	Transformed function
$f(y) = u(y) \pm w(y)$	$F(k) = U(k) \pm W(k)$
$f(y) = \frac{d^n u(y)}{dy^n}$	$F(k) = \frac{(k+n)!}{k!} U(k+n)$
$f(y) = u^2$	$F(k) = \sum_{r=0}^k U(r)U(k-r)$
$f(y) = \left(\frac{du(y)}{dy}\right)^2$	$F(k) = \sum_{r=0}^k (r+1)(k-r+1)U(r+1)U(k-r+1)$
$f(y) = \left(\frac{d^2u(y)}{dy^2}\right)^2$	$F(k) = \sum_{r=0}^k (r+1)(r+2)(k-r+1)(k-r+2)U(r+2)U(k-r+2)$

**Table 1.**  
 Operations and properties of differential transform method.

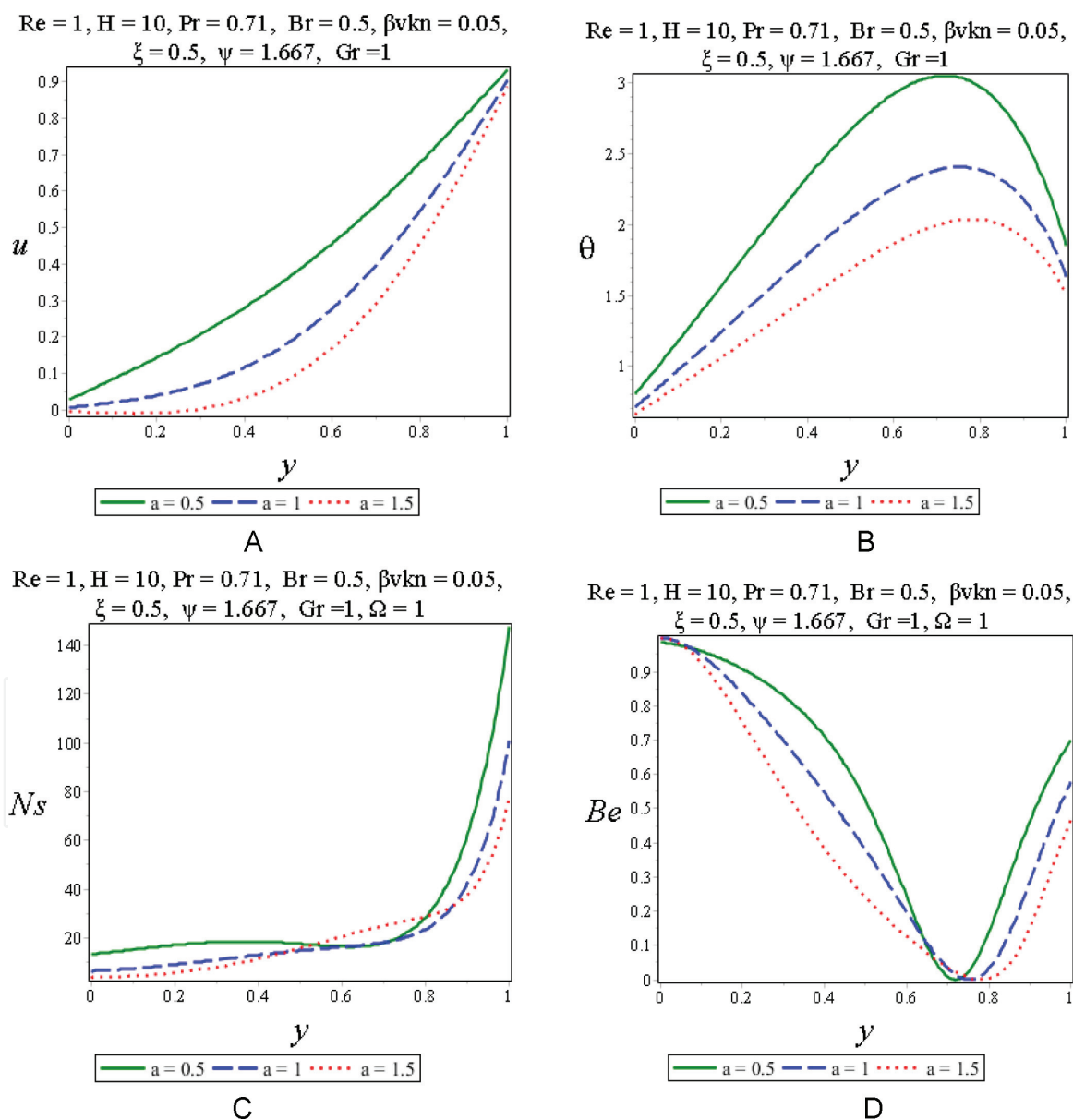


**Figure 2.**  
 A. Couple stress parameter vs. fluid velocity. B. Couple stress parameter vs. fluid temperature. C. Couple stress parameter vs. entropy generation. D. Couple stress parameter vs. Bejan number.

$$\Theta(k+2) = \frac{1}{(k+2)!} \left[ \text{RePr}(k+1)\Theta(k+1) - Br \left( \sum_{r=0}^k (r+1)F(r+1) \right. \right. \\ \left. \left. - \frac{Br}{a^2} \left( \sum_{r=0}^k (r+1)(r+2)F(r+2)(k-r+1)(k-r+2)F(k-r+2) \right) \right. \right. \\ \left. \left. - BrH^2 \left( \sum_{r=0}^k F(r)F(k-r) \right) \right] \quad (13)$$

where  $F(k)$  and  $\Theta(k)$  are the transformed functions of  $f(y)$  and  $\theta(y)$ , respectively. These are given by

$$f(y) = \sum_{k=0}^{\infty} y^k F(k), \theta(y) = \sum_{k=0}^{\infty} y^k \Theta(k). \quad (14)$$

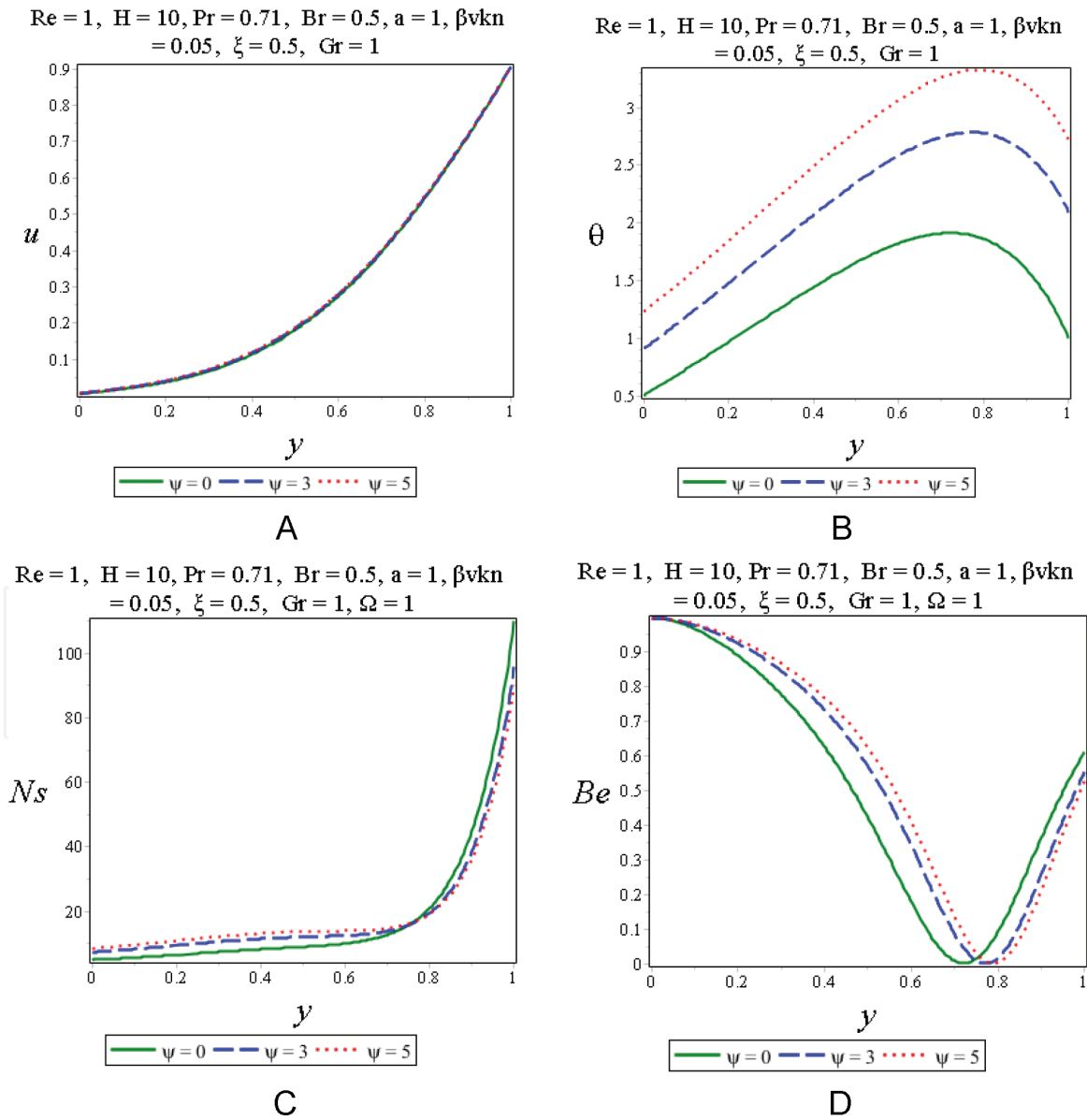


**Figure 3.** A. Fluid wall interaction parameter vs. fluid velocity. B. Fluid wall interaction parameter vs. fluid temperature. C. Fluid wall interaction parameter vs. entropy generation. D. Fluid wall interaction vs. Bejan number.



Using the recursive relations of Eqs. (12) and (13), we can obtain the differential coefficients,  $F(4), F(5), \dots, F(n)$  and  $\Theta(4), \Theta(5), \Theta(n)$  by setting  $k = 0, 1, 2, \dots$ . The values of  $F(j)$  for  $j = 4, 5, \dots$  and  $\Theta(j)$  for  $j = 2, 3, \dots$  can now be evaluated in terms of  $F(0), F(1), F(2), F(3), \Theta(0)$  and  $\Theta(1)$ . For convenience, the values of  $F(0), F(1), F(2), F(3), \Theta(0)$  and  $\Theta(1)$  are set as unknowns such as

$$\begin{aligned} F(0) &= a_1, & F(1) &= a_2, & F(2) &= a_3, & F(3) &= a_4, \\ \Theta(0) &= b_1, & \Theta(1) &= b_2. \end{aligned} \quad (15)$$

The values of  $F(k)$  and  $\Theta(k)$  for  $k = 0, 1, \dots$  are now substituted back into Eq. (14) to obtain the series solutions in the form:

$$f(y) = \sum_{k=0}^n y^k F(k), \quad \theta(y) = \sum_{k=0}^n y^k \Theta(k). \quad (16)$$

We next invoke the transformed form of boundary condition (8) on (16) to determine the values of all the unknown coefficients stated in (15). Coding

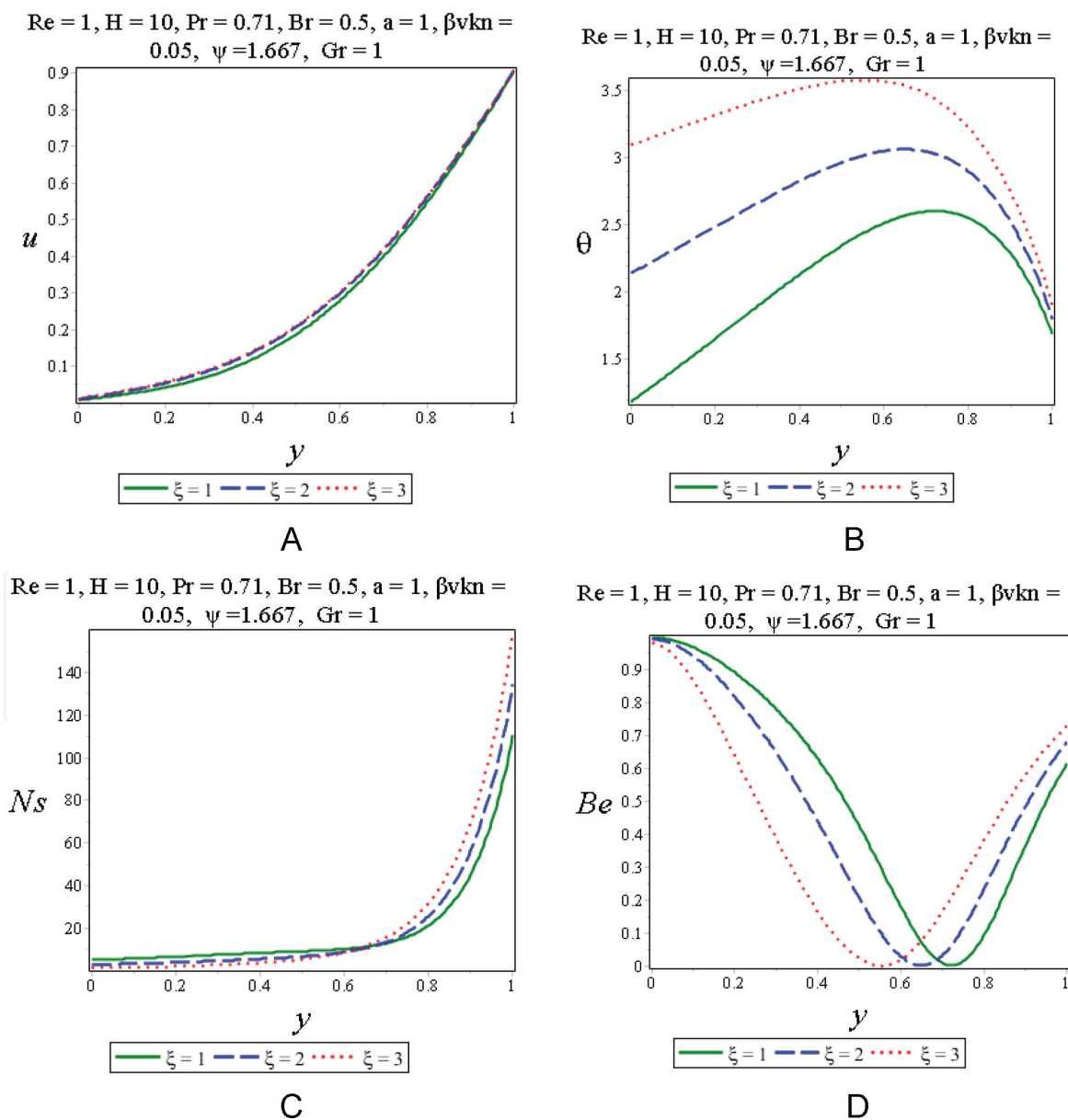


**Figure 4.**  
 A. Effective temperature ratio vs. fluid velocity. B. Effective temperature ratio vs. fluid temperature. C. Effective temperature ratio vs. entropy generation. D. Effective temperature ratio vs. Bejan number.



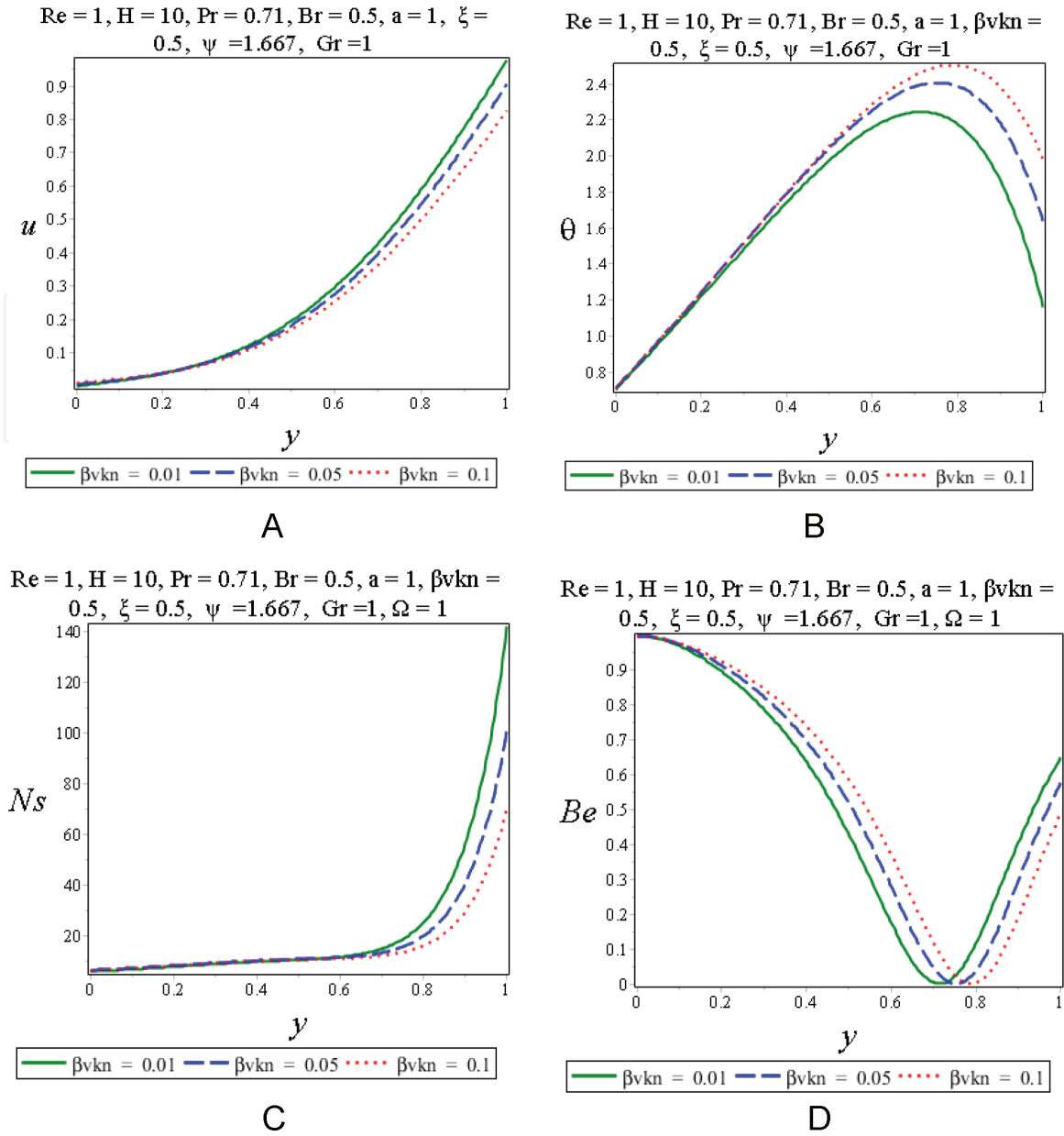


**Figure 5.** A. Rarefaction vs. fluid velocity. B. Rarefaction vs. fluid temperature. C. Rarefaction vs. entropy generation. D. Rarefaction vs. Bejan number.

Eqs. (12)–(15) in symbolic Maple software yields the approximate solution. The results are presented in **Figures 2–6**.

To verify the accuracy of the results, the exact solution of the velocity profile (6) subject to the boundary conditions (8) at  $\beta v Kn = 0.05, Gr = 0, a = 1, Re = 0.1, H = 1$  is obtained as.

$$\begin{aligned}
 u(y) = & (-3.063639 e^{(0.866146y)} + 2.057901 \text{Cos} [0.470472y] + \\
 & 1. e^{(1.732291y)} \text{Cos} [0.528272y] + 1.808594 \text{Sin} [0.4704729y] - \\
 & 0.093418 e^{(1.732291y)} \text{Sin} [0.528272y])
 \end{aligned} \tag{17}$$

The above solution is compared with DTM solution as displayed in **Table 2**.

### 3.2 Analysis of entropy generation

The local entropy generation for the flow is given as Bejan [13]:

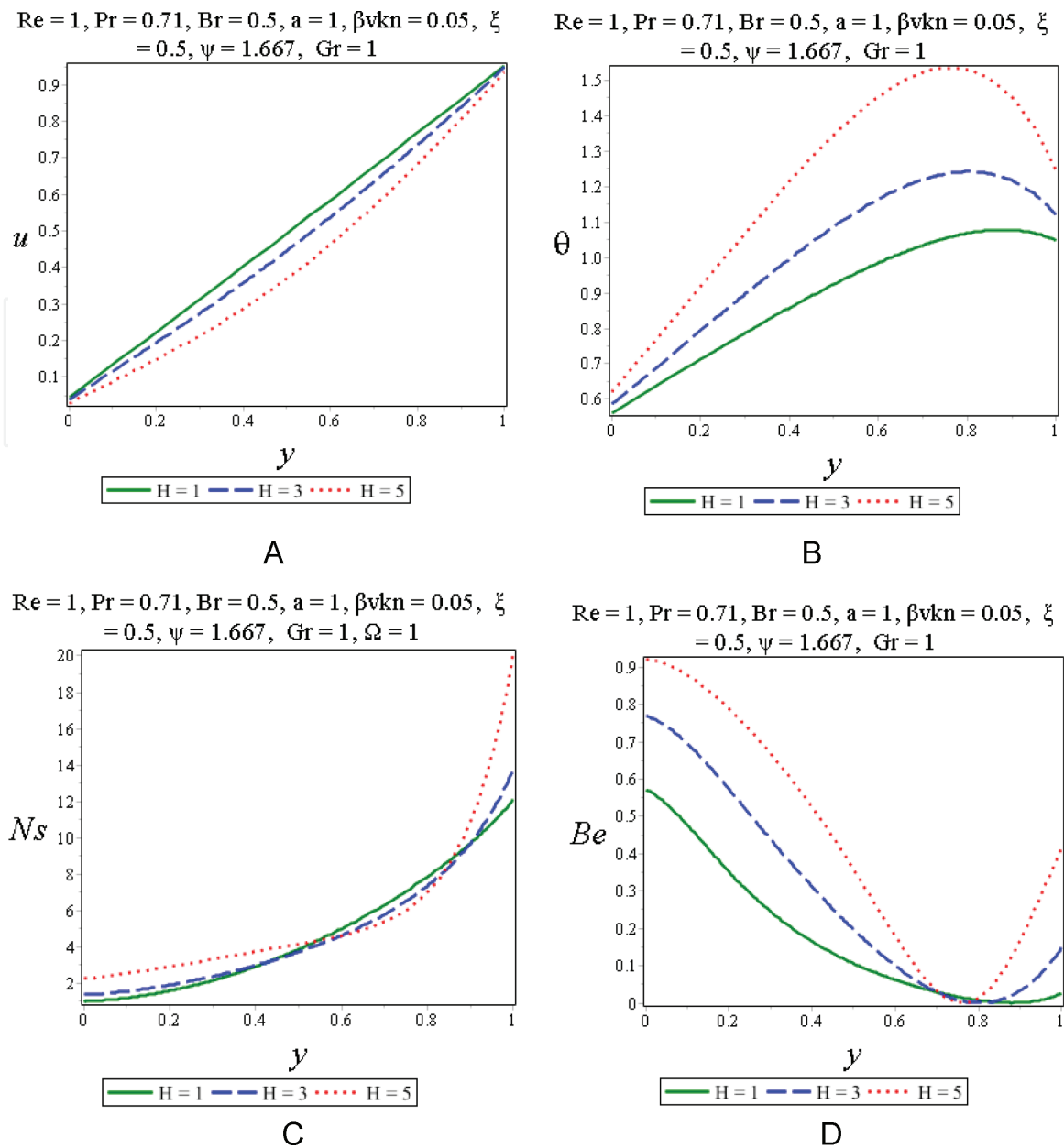


**Figure 6.** A. Hartmann Number vs. fluid velocity. B. Hartmann Number vs. fluid temperature. C. Hartmann Number vs. entropy generation. D. Hartmann Number vs. Bejan number.

$$S_G = \frac{k}{T_0^2} \left( \frac{dT^*}{dy^*} \right)^2 + \frac{\mu}{T_0} \left( \left( \frac{du^*}{dy^*} \right)^2 \right) + \frac{1}{a^2} \left( \left( \frac{d^2u}{dy^2} \right)^2 \right) + \frac{\sigma B_0^2}{T_0} u^{*2}. \quad (18)$$

The first term in Eq. (18)  $\frac{k}{T_0^2} \left( \frac{dT^*}{dy^*} \right)^2$  is entropy generation due to heat transfer; the next term  $\frac{\mu}{T_0} \left( \left( \frac{du^*}{dy^*} \right)^2 \right)$  is entropy generation due to viscous dissipation,  $\frac{1}{a^2} \left( \left( \frac{d^2u}{dy^2} \right)^2 \right)$  and  $\frac{\sigma B_0^2}{T_0} u^{*2}$  are couple stress and magnetic entropy generation.

Using (4) in Eq. (18), the dimensionless form of entropy generation is written as

$$Ns = \left( \frac{d\theta}{dy} \right)^2 + \frac{Br}{\Omega} \left( \left( \frac{du}{dy} \right)^2 \right) + \frac{Br}{\Omega a^2} \left( \left( \frac{d^2u}{dy^2} \right)^2 \right) + \frac{BrM^2}{\Omega} u^2, \quad (19)$$

$\beta\nu Kn = 0.05, Gr = 0, a = 1, Re = 0.1, H = 1$		
$y$	Exact	DTM
0	0.001872811813791	0.001872811814000
0.1	0.005546352540252	0.005546352541866
0.2	0.008819633339440	0.008819633342380
0.3	0.011379286267087	0.011379286271194
0.4	0.013003721837660	0.013003721842694
0.5	0.013560741309568	0.013560741315200
0.6	0.013006153436252	0.013006153442060
0.7	0.011383386215798	0.011383386221257
0.8	0.008824085393964	0.008824085398432
0.9	0.005549692555064	0.005549692557769
1	0.001873996484802	0.001873996484819

**Table 2.**  
Comparison of the exact solution with the values of velocity ( $u$ ).

where  $(S_G, N_s)$  are the dimensional and dimensionless entropy generation rates. The ratio of heat transfer entropy generation ( $N_1$ ) to fluid friction entropy generation ( $N_2$ ) is represented as

$$\Phi = \frac{N_2}{N_1} \tag{20}$$

Alternatively, Bejan number gives the entropy generation distribution ratio parameter; it represents the ratio of heat transfer entropy generation ( $N_1$ ) to the total entropy generation ( $N_s$ ) due to heat transfer and fluid friction; it is defined as

$$Be = \frac{N_1}{N_s} = \frac{1}{1 + \Phi}, \tag{21}$$

$$Be = \begin{cases} 0, N_2 \gg N_1 \\ 0.5, N_1 = N_2 \\ 1, N_2 \ll N_1 \end{cases} \tag{22}$$

Note that  $N_1$  represents heat transfer irreversibility, while  $N_2$  denotes irreversibility due to viscous dissipation, couple stresses and magnetic field.

#### 4. Results and discussion

In this work, investigation has been conducted on fully developed, steady, viscous and incompressible flow of couple stress fluid in a vertical micro-porous-channel in the presence of magnetic field. Effects of couple stress parameter ( $a$ ), fluid wall interaction parameter ( $\psi$ ), effective temperature ratio (ETR) ( $\xi$ ), rarefaction ( $\beta\nu Kn$ ) and Hartmann number ( $H$ ) are presented in this section. Reasonable intervals for the above parameters as used by Chen and Weng [32] are adopted in this investigation:  $0 \leq H \leq 10$ ,  $0 \leq \beta\nu Kn \leq 0.1$ ,  $0 \leq \psi \leq 10$  and the selected reference values of  $\beta\nu Kn = 0.05$ ,  $\ln = 1.667$ . Furthermore,  $0 \leq \xi \leq 5$  and  $0 \leq a \leq 2$  with reference values of  $a = 1$ ,  $\xi = 0.5$ .

#### 4.1 Influence of couple stress parameter

**Figure 2A** illustrates the influence of couple stress parameter on fluid velocity. The plot shows a significant reduction in fluid velocity as the values of couple stress parameter increase. This observation is due to the increase in the dynamic viscosity of the fluid. In **Figure 2B**, it is illustrated that fluid temperature drops as couple stress parameter increases. It is depicted in **Figure 2C** that fluid entropy generation decreases at the microchannel walls as couple stress parameter increases. However, the effect is opposite near the middle of the microchannel. The same scenario is observed in **Figure 2D**; it is shown that Bejan number reduces in value at microchannel right wall which is an indication that fluid friction irreversibility is the major contributor to entropy generation as couple stress parameter increases.

#### 4.2 Influence of fluid-structure interaction parameter

**Figure 3A** presents the effect of fluid-structure interaction parameter on fluid velocity. It is noted that FSIP does not have any significant effect on the slip velocity at the walls as well as the microchannel. However, **Figure 3B** reveals that fluid temperature is enhanced as FSIP increases. Response to the enhancement in fluid temperature in **Figure 3B** is the rise in fluid entropy generation at the hotter wall of the microchannel, while entropy generation is reduced at the cooler wall as depicted in **Figure 3C**. In **Figure 3D**, it is noticed that Bejan number increases at the hotter wall of the microchannel, while it reduces at the cooler wall. The implication of the latter is that heat transfer irreversibility is the cause of entropy generation at the hotter wall, while on the other hand, fluid friction irreversibility is the major contributor at the cooler wall of the microchannel.

#### 4.3 Influence of effective temperature ratio

Next is the response of fluid velocity, fluid temperature and entropy generation to variation in effective temperature ratio. In **Figure 4**, it is observed that velocity is accelerated slightly except towards the microchannel centre and plate  $y = 0$ . In **Figure 4B**, fluid temperature is significantly enhanced at increasing values of effective temperature ratio. The effect of this is noticed in **Figure 4C** with an increase in entropy production approaching the microchannel plate  $y = 1$ . Furthermore, Bejan number rises approaching the plate  $y = 1$  but reduces towards  $y = 0$  in **Figure 4D**. It is then concluded that fluid friction irreversibility is dominant at plate  $y = 0$ , while heat transfer irreversibility is dominant at plate  $y = 1$ .

#### 4.4 Influence of rarefaction

In **Figure 5A**, the effect of rarefaction parameter on fluid velocity is presented. The plot indicates that rarefaction parameter increases and fluid velocity at plate  $y = 0$  is not significant; however, it is decelerated towards the microchannel plate  $y = 1$ . Fluid temperature is considerably enhanced at plate  $y = 1$  for different values of rarefaction as displayed in **Figure 5B**. **Figures 5C** and **5D** presents similar results at plate  $y = 1$ . Both entropy generation and Bejan number reduce as the values of rarefaction parameter increase. The implication of this observation is that entropy generation at microchannel wall  $y = 1$  is a consequence of viscous dissipation.

#### 4.5 Influence of Hartmann number

Finally, the response of fluid velocity, temperature, entropy generation and Bejan number to variation in Hartmann number is presented in **Figure 6**. In **Figure 6A**, fluid velocity is found to have decelerated within the microchannel region. The observed reduction in the motion of fluid is attributed to the presence of applied magnetic field which usually induces a resistive type of force known as Lorentz force. Also the presence of Ohmic heating in the flow significantly enhanced fluid temperature as depicted in **Figure 6B**. **Figures 6C** and **6D** displays increase in fluid entropy generation and Bejan number at the microchannel walls as Hartmann number increases from 1 to 5. It is deduced that fluid entropy generation is induced by heat transfer irreversibility.

### 5. Conclusions

Entropy generation of fully developed steady, viscous, incompressible couple stress fluid in a vertical micro-porous-channel in the presence of magnetic field is analysed in this work. The equations governing the fluid flow are solved via an efficient technique proposed by Zhou. Then fluid entropy generation and Bejan number are calculated by the results obtained. This work reduces to Chen and Weng [34] when Hartmann number, couple stress parameter, entropy generation and Bejan number are neglected ( $H \rightarrow 0, a \rightarrow 0, Ns \rightarrow 0, Be \rightarrow 0$ ). Furthermore, it agrees with Jha and Aina [10] in the absence of couple stress parameter, entropy generation and Bejan number ( $a \rightarrow 0, Ns \rightarrow 0, Be \rightarrow 0$ ). The present study is significant in the cooling of microchannel devices and conservation of useful energy. The following conclusions are made based on the results above:

1. Couple stress parameter reduces fluid velocity, velocity slip, temperature and entropy generation.
2. Increase in fluid-structure interaction parameter increases fluid temperature. However, entropy generation enhances at the hotter wall and reduces at the cooler region of the microchannel. Furthermore, fluid irreversibility is enhanced at the hot wall and increases at the cold wall.
3. Effective temperature ratio slightly enhances fluid velocity and velocity slip, raising fluid temperature significantly.
4. An increase in the values of rarefaction mainly reduces fluid velocity and velocity slip, increases fluid temperature and reduces entropy generation.
5. Hartmann number decreases fluid velocity and velocity slip, while the temperature is enhanced considerably. Entropy generation and Bejan number are enhanced at microchannel walls.

### Acknowledgements

Authors appreciate the funding provided by Covenant University, Ota.

## Nomenclature

$B_0$	uniform magnetic field
$u$	fluid velocity
$h$	channel width
$f_t, f_v$	thermal and tangential momentum accommodation coefficients, respectively
$C_p$	specific heat capacity
Re	Reynolds number
$a$	couple stress parameter
$k$	thermal conductivity
Kn	Knudsen number
$H$	Hartmann number
Pr	Prandtl number
$T$	temperature of fluid
$T_0$	reference temperature
$Br$	Brinkman number
$E_G$	local volumetric entropy generation rate
$Be$	Bejan number
$C_v$	specific heats at constant volume
$N_s$	dimensionless entropy generation parameter

## Greek letters


$\rho$	fluid density
$\beta_t, \beta_v$	dimensionless variables
$\gamma_s$	ratio of specific heat
$\mu$	dynamic viscosity
$\xi$	effective temperature ratio
$\sigma$	electrical conductivity
$\Omega$	temperature difference
$\eta$	fluid particle size effect due to couple stresses
$\psi$	fluid wall interaction parameter

## Author details

Abiodun A. Opanuga\*, Olasunmbo O. Agboola, Hilary I. Okagbue and Sheila A. Bishop  
Department of Mathematics, Covenant University, Ota, Nigeria

\*Address all correspondence to: [abiodun.opanuga@covenantuiversity.edu.ng](mailto:abiodun.opanuga@covenantuiversity.edu.ng)

## IntechOpen

© 2018 The Author(s). Licensee IntechOpen. This chapter is distributed under the terms of the Creative Commons Attribution License (<http://creativecommons.org/licenses/by/3.0>), which permits unrestricted use, distribution, and reproduction in any medium, provided the original work is properly cited. 



## References

- [1] Agboola OO, Opanuga AA, Okagbue HI, Bishop SA, Ogunniyi PO. Analysis of hall effects on the entropy generation of natural convection flow through a vertical microchannel. *International Journal of Mechanical Engineering and Technology*. 2008;**9**(8):712-721
- [2] Arkilic EB, Schmidt MA, Breuer KS. Gaseous slip flow in long microchannels. *Journal of Microelectromechanical Systems*. 1997;**6**:167-178
- [3] Sofonea V, Sekerka RF. Diffuse-reflection boundary conditions for a thermal lattice Boltzmann model in two dimensions: Evidence of temperature jump and slip velocity in microchannels. *Physical Review E – Statistical Nonlinear and Soft Matter Physics*. 2005;**71**:1-10 <http://dx.doi.org/10.1103/PhysRevE.71.066709>
- [4] Lv Q, Liu X, Wang E, Wang S. Analytical solution to predicting gaseous mass flow rates of microchannels in a wide range of Knudsen numbers. *Physical Review E*. 2013;**88**:013007 <http://dx.doi.org/10.1103/PhysRevE.88.013007>
- [5] Khadrawi AF, Al-Shyyab A. Slip flow and heat transfer in axially moving micro-concentric cylinders. *International Communications in Heat and Mass Transfer*. 2010;**37**:1149-1152 <http://dx.doi.org/10.1016/j.icheatmasstransfer.2010.06.006>
- [6] Chen S, Tian Z. Simulation of thermal micro-flow using lattice Boltzmann method with Langmuir slip model. *International Journal of Heat and Fluid Flow*. 2010;**31**:227-235 <http://dx.doi.org/10.1016/j.ijheatfluidflow.2009.12.006>
- [7] Larrode FE, Housiadas C, Drossinos Y. Slip-flow heat transfer in circular tubes. *International Journal of Heat and Mass Transfer*. 2000;**43**:2669-26680
- [8] Adesanya SO. Free convective flow of heat generating fluid through a porous vertical channel with velocity slip and temperature jump. *Ain Shams Engineering Journal*. 2015;**6**:1045-1052. DOI: <http://dx.doi.org/10.1016/j.asej.2014.12.008>
- [9] Aziz A, Niedbalski N. Thermally developing microtube gas flow with axial conduction and viscous dissipation. *International Journal of Thermal Sciences*. 2011;**50**:332-340 <http://dx.doi.org/10.1016/j.ijthermalsci.2010.08.003>
- [10] Jha BK, Aina B. MHD natural convection flow in a vertical porous microchannel formed by nonconducting and conducting plates in the presence of induced magnetic field. *Heat Transfer Research*. 2017;**48**(15):1-24
- [11] Jha BK, Aina B, Joseph SB. Natural convection flow in a vertical microchannel with suction/injection. *Proceedings of the Institution of Mechanical Engineers, Part E: Journal of Process Mechanical Engineering*. 2014; **228**(3):171-180. DOI: 10.1177/0954408913492719
- [12] Jha BK, Aina B, Ajiya AT. MHD natural convection flow in a vertical parallel plate microchannel. *Ain Shams Engineering Journal*. 2015;**6**:289-295
- [13] Bejan A. *Entropy Generation through Heat and Fluid Flow*. New York: Wiley; 1982
- [14] Adesanya SO, Falade JA, Jangili S, Beg OA. Irreversibility analysis for reactive third-grade fluid flow and heat transfer with convective wall cooling. *Alexandria Engineering Journal*. 2017; **56**:153-160
- [15] Adesanya SO, Kareem SO, Falade JA, Arekete SA. Entropy generation analysis for a reactive couple stress fluid

flow through a channel saturated with porous material. *Energy*. 2015;**93**: 1239-1245

[16] Jangili S, Adesanya SO, Falade JA, Gajjela N. Entropy generation analysis for a radiative micropolar fluid flow through a vertical channel saturated with non-Darcian porous medium. *International Journal of Applied and Computational Mathematics*. **3**(4): 3759-3782. DOI: 10.1007/s40819-017-0322-8

[17] Adesanya SO, Makinde OD. Irreversibility analysis in a couple stress film flow along an inclined heated plate with adiabatic free surface. *Physica A: Statistical Mechanics and its Applications*. 2015;**432**:222-229

[18] Adesanya SO, Makinde OD. Effects of couple stresses on entropy generation rate in a porous channel with convective heating. *Computational & Applied Mathematics*. 2015;**34**:293-307. DOI: 10.1007/s40314-014-0117-z

[19] Ajibade AO, Jha BK, Omame A. Entropy generation under the effect of suction/injection. *Applied Mathematical Modelling*. 2011;**35**:4630-4646

[20] Eegunjobi AS, Makinde OD. Effects of Navier slip on entropy generation in a porous channel with suction/injection. *Journal of Thermal Science and Technology*. 2002;**7**(4): 522-535

[21] Eegunjobi AS, Makinde OD. Combined effect of buoyancy force and Navier slip on entropy generation in a vertical porous channel. *Entropy*. 2012; **14**:1028-1044. DOI: 10.3390/e14061028

[22] Das S, Jana RN. Entropy generation due to MHD flow in a porous channel with Navier slip. *Ain Shams Engineering Journal*. 2014;**5**:575-584

[23] Opanuga AA, Okagbue HI, Agboola OO, Imaga OF. Entropy generation analysis of buoyancy effect on hydromagnetic poiseuille flow with internal heat generation. *Defect and Diffusion Forum*. 2017;**378**:102-112

[24] Opanuga AA, Gbadeyan JA, Iyase SA. Second law analysis of hydromagnetic couple stress fluid embedded in a non-Darcian porous medium. *IAENG International Journal of Applied Mathematics*. 2017;**47**(3): 287-294

[25] Opanuga AA, Okagbue HI, Agboola OO. Irreversibility analysis of a radiative MHD Poiseuille flow through porous medium with slip condition. *Proceedings of The World Congress on Engineering 2017*; July 5–7; London, U.K

[26] Opanuga AA, Bishop SA, Okagbue HI, Agboola OO. Hall current and joule heating effects on flow of couple stress fluid with entropy generation. *Engineering, Technology & Applied Science Research*. 2008;**8**(3):2923-2930

[27] Arikoglu A. Ozkol solution of difference equations by using differential transform method. *Applied Mathematics and Computation*. 2006; **173**(1):126-136. <http://dx.doi.org/10.1016/j.amc.2005.06.013>

[28] Biazar J, Eslami M. Differential transform method for quadratic Riccati differential equation. *International Journal of Nonlinear Science*. 2010;**9**(4): 444-447

[29] Agboola OO, Gbadeyan JA, Opanuga AA, Agarana MC, Bishop SA, Oghonyon JG. Variational iteration method for natural frequencies of a cantilever beam with special attention to the higher modes. *Proceedings of The World Congress on Engineering 2017*; July 5–7 London; UK

[30] Agboola OO, Opanuga AA, Gbadeyan JA. Solution of third order

ordinary differential equations using differential transform method. *Global Journal of Pure and Applied Mathematics*. 2015;**11**(4):2511-2517

[31] Odibat Z. Differential transform method for solving Volterra integral equation with separable kernels. *Mathematical and Computer Modelling*. 2008;**48**:144-149. <http://dx.doi.org/10.1016/j.mcm.2007.12.022>

[32] Opanuga AA, Agboola OO, Okagbue HI. Approximate solution of multipoint boundary value problems. *Journal of Engineering and Applied Sciences*. 2015; **10**(4):85-89

[33] Opanuga AA, Okagbue HI, Agboola OO, Bishop SA. Second law analysis of ion slip effect on MHD couple stress fluid. *International Journal of Mechanics*. 2018;**12**:96-101

[34] Chen CK, Weng HC. Natural convection in a vertical microchannel. *Journal of Heat Transfer*. 2005;**127**: 1053-1056

IntechOpen